Retrospective Data-driven Respiratory Gating for PET using TOF Information

Mengdie Wang [1,2], Ning Guo[2], Hui Zhang[1], Georges Elfhakri[2], Guangshu Hu[1], Quanzheng Li[2]

Abstract— **Traditional data-driven respiratory gating method is capable of detecting breathing cycles directly from positron emission tomography (PET) data, but usually fails at low SNR, particularly at low dose PET/CT study. Time-of-flight (TOF) PET has the potential to improve the SNR. In order for TOF information to reduce the statistical noise and boost the performance of respiratory gating, we present a robust data-driven respiratory gating method using TOF information, which retrospectively derived the respiratory signal from the acquired TOF-PET data. The PET data was acquired in list mode format and analyzed in sinogram space. The method was demonstrated with patient datasets acquired on a TOF PET/CT system. Data-driven gating methods by center of mass (COM) and principle component analysis (PCA) algorithm were successfully performed on nonTOF PET and TOF PET dataset. To assess the accuracy of the data-driven respiratory signal, a hardware-based signal was acquired for comparison. The study showed that retrospectively respiratory gating using TOF sinograms has improved the SNR, and outperforms the non-TOF gating under both COM and PCA algorithms.**

I. Introduction

Respiratory motion in PET acquisition will significantly lower the resolution of the image, leading to poor detectability of tumors, incorrect standard uptake value (SUV) calculation, inaccurate PET-measured tumor volume, and reduced accuracy in the localization of PET abnormalities [1-6]. However, respiratory gating helps to mitigate the negative effect of respiratory motion in the images [7]. Several technical strategies have been developed to implement respiratory gating [8-12] based on the chest wall excursion [13, 14]. However, these techniques assume that the measured parameter serves as a surrogate estimate of the respiratory phase of a moving region. Yet, in practice, the respiratory state estimation is not always accurate [15].

An alternative approach called data-driven gating technique, which uses the emission data itself to estimate the respiratory motion, can be employed in respiratory gating of PET. This method can provide a direct estimate of the respiratory signal of an imaged region from analysis of the region itself. A number of methods have been proposed for data-driven gating, such as the Center-of-Mass method (COM) [16, 17] and Principal Component Analysis (PCA) method [18], Sensitivity method (SENS) [19], the Spectral Analysis method (SAM) [20] and Combining Signal Fluctuations [21]. However, these methods require a fine temporal scale to guarantee enough samples and fail at low signal-to-noise ratio (SNR), particularly at low dose PET/CT study. Since low dose study is an extremely popular topic nowadays, several approaches have been proposed to improve the SNR of PET under low dose, such as the development of new detectors and advanced electronics, the evolution of 3D PET systems and the new information gained by the use of time-of-flight (TOF) technology [22]. For TOF-PET, a Fourier Rebinning method of Time-of-flight (FORET), has been derived that converts TOF sinogram to nonTOF sinogram while retaining the SNR advantages of the TOF information [23, 24], which can potentially improve the performance of traditional data-driven respiratory gating.

In this work, we present a novel method combing FORET and data-driven technique for human respiratory gating. In this method, 3D TOF PET data is rebinned into 2D nonTOF data without loss of TOF information. We evaluate the performance of TOF PET data-driven gating compared with the hardware-based signal and nonTOF PET data-driven signal using both COM and PCA algorithm. We also demonstrate the advantage of the TOF technique in low dose PET/CT study.

II. Methods

In our TOF automatic gating method, we first split the TOF PET list mode data into coarse TOF sinograms with 100ms duration and post-process these sinograms to achieve FORET sinograms. Then the COM and PCA methods were applied to the sinograms as regular nonTOF method and the raw respiratory signal was consequently extracted, followed by Gaussian bandpass filtering. Finally, we assessed the robustness of data-driven respiratory gating by correlation analysis with hardware-based signal as the gold standard. The flow diagram of this work is shown in Fig. 1.

A. Experimental Setup

To evaluate the presented method, a 5min chest PET/CT scan by Siemens Biograph mCT was performed 90min after injection of 6mCi 18F-FDG in a human subject. TOF PET list mode data with 580ps timing resolution was stored and the respiratory data was acquired simultaneously using Anzai AZ-733 system. We obtained the data-driven signals with and without TOF information. In this study, the emission coincidence rate was 141 kcps, with 36 million prompt events collected within 5 minutes. Following the acquisition, an optimal FORET was applied to PET

This work was supported in part by the scholarship from China Scholarship Council (CSC, No. 201306210270).

[1]Department of Biomedical Engineering, Tsinghua University, Beijing, 100084, China. M. Wang is also with the Division of Nuclear Medicine and Molecular Imaging, Department of Radiology, Massachusetts General Hospital, Harvard Medical School, Boston, MA 02114, USA. Contact: mwang20@mgh.harvard.edu

[2]Division of Nuclear Medicine and Molecular Imaging, Department of Radiology, Massachusetts General Hospital, Harvard Medical School, Boston, MA 02114, USA.

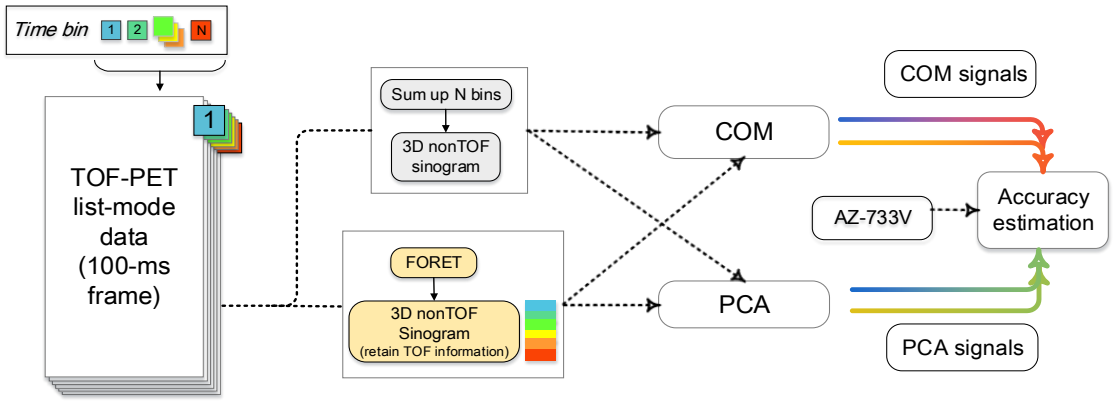

Fig. 1. Flow diagram representation of the steps involved in data-driven respiratory gating using TOF and nonTOF data.

listmode data to rebin the 3D TOF sinograms to 2D nonTOF data using FORET. The nonTOF PET sinogram data was approximately obtained by summing the TOF sinogram data in TOF bin direction. Oblique coincidence events, that is, coincidences between detectors located on different rings, were rebinned into the 109 transverse sinograms of the Biograph mCT scanner with the help of Single Slice Rebinning (SSRB) algorithm, rebinning the 3D sinograms to lower dimensional format[25]. As a result of FORET, the 55th slice out of 109 slices of both nonTOF and FORET sinograms sorted from list mode data are shown in Fig.2. The improvement of SNR by TOF information was obviously observed in the sinograms.

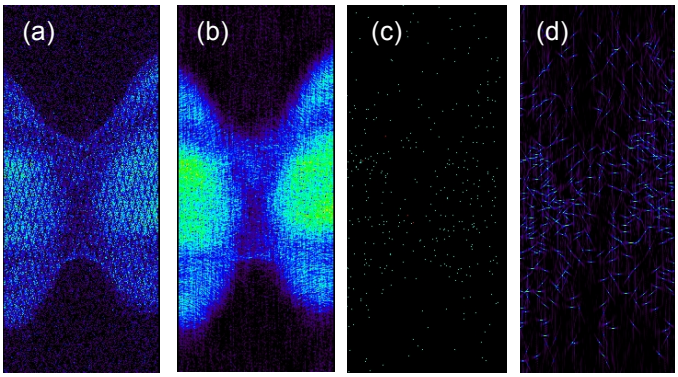

Fig. 2. 2D Sinogram data. (a) 1 min nonTOF (b) 1 min FORET (c) 100 ms nonTOF (d) 100 ms FORET.

B. Algorithm

As the most crucial algorithm applied in this work, FORET-2D (FORET to 2D non time-of- flight) converts 3D TOF data $\mathcal{P}(\omega_s,k,z,\delta;\omega_t)$ to 2D nonTOF data $\mathcal{P}(\omega_s,k,z,0;0)$ while retaining the SNR advantages of the TOF information. The approximate rebinning equation can be written as [23],

$$\mathcal{P}(\omega_s,k,z,0;0) \approx \frac{1}{\sqrt{1+\delta^2}}\{H(0)/H(\omega_t)\}\psi$$
$$\psi = e^{-ik(\frac{\omega_t\sqrt{1+\delta^2}}{\omega_s})}\,\mathcal{P}(\omega_s,k,z,z+\frac{\delta k}{\omega_s},\delta;\omega_t) \quad (1)$$

where $\mathcal{P}$ is the 3D Fourier transform of $p(s,\phi,z,\delta;t)$ in the radial coordinates s, the angular coordinates ϕ and the TOF variable t, z is the axial midpoint of each line of response (LOR), δ is the tangent of the oblique angle, ω_s, ω_t and k are the frequency variables corresponding to s, t and ϕ. Note that H is the Fourier transforms of the TOF kernel h. This rebinning equation results in negligible bias and the approximation error is large when ω_s is small. We apply this algorithm to estimate 2D sinogram from 3D TOF data $\mathcal{P}(\omega_s,k,z,\delta;\omega_t)$.

Based on the 2D sinograms obtained after SSRB and FORET (for nonTOF and TOF data respectively), two gating methods (COM and PCA) were applied to extract the respiratory signal.

COM method is based on a direct estimation of the motion inside the field of view. For this method, the coincidence counting rate per 100ms frame was determined from the processed sinogram as a function of the axial coordinate (slice number). SSRB algorithm enables an axial assignment of coincidence events along the scanner's z-axis. As activity inside the thorax moves along the axis due to respiratory motion, the axial component of sinogram contains information about the respiratory phase. To extract this information, we compute the axial center of mass as a function of time frame:

$$COM(t) = \frac{\sum_i i.M(i,t)}{\sum_i M(i,t)} \quad (2)$$

where $M(i,t)$ is an axial histogram (t: time frame; i: slice number; i = 1,…,47) of measured true events within

time frame t. The results of the COM computation over time should resemble a somewhat sinusoidal waveform representative of the cyclic respiratory pattern. However, due to statistical fluctuations as well as the translations of the heart during the cardiac contraction, the COM signal contains a signal not only at the respiratory rate, but also a strong component due to the heartbeat. To extract more accurate respiratory motion information, we applied a low-pass filter using a Gaussian kernel with a standard deviation of 0.5sec.

PCA is a simple, non-parametric method to extract a lower dimension feature space (orthogonal components) from the original data space with a huge dimension. When the observed variables are highly correlated, PCA provides an alternative way to describe the data economically with high accuracy. In this paper, we utilized PCA to detect the variation in dynamic sinogram sorted from list mode PET data. Assume that s_i is dynamic sinogram (i runs from 1 to N), which can be written as a linear combination as

$$s_i \approx \bar{s} + \sum_{k=1}^{K} \omega_{ik} c_k \qquad (3)$$

where $\bar{s}$ is the mean of the data, c_k the principal components (PCs) with the same dimension as s_i and ω_{ik} the weight factors. If the dynamic data s_i is affected by motion, it is to be expected that the first component will contain motion information, according to PCA [26]. Considering that the components c_k are orthogonal basis vectors, the weight factors ω_{ik} can be obtained as

$$\omega_{ik} = c_k.(s_i - \bar{s}) \qquad (4)$$

By doing so, we can extract the maximum variation from dynamic sinograms s_i. However, due to the high temporal resolution required by data-driven auto-gating, before applying this technique on PET sinograms, we unlist data into low spatial resolution dynamic sinograms while keeping axial resolution. After that, we scaled sinograms for decay correction considering the dynamic behavior of tracer. Finally, PCA was used to extract the gating signal. These computations resulted in raw respiration curve (the first component) that was filtered in the same way afterwards as described above.

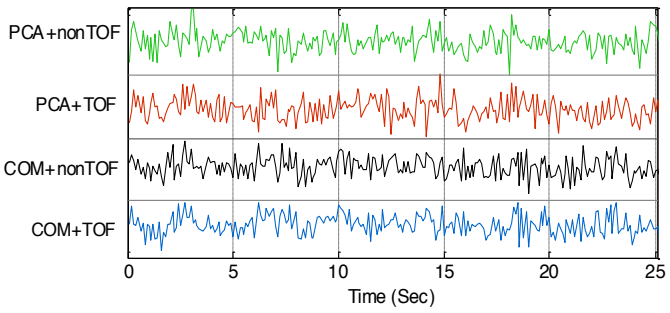

Fig. 3 raw data (mean corrected) representing respiratory signal computed by COM and PCA algorithms (showing 25 seconds out of 5 min).

TABLE I. ACCURACY FOR EACH SIGNAL ESTIMATED USING THE FOUR METHODS

	Trace Correlation	Δt≥400ms (%)	Trigger Error (ms)
NonTOF+PCA	0.60	30.77%	1.89+4.25
NonTOF+COM	0.80	11.54%	0.99+2.38
TOF+PCA	0.73	7.69%	1.52+3.12
TOF+COM	0.83	3.84%	0.14+3.53

III. RESULTS AND DISCUSSION

Fig. 3 demonstrates the raw data (mean corrected) representing respiratory signal computed by COM and PCA algorithms. Note that only a small segment of the data (25 sec out of 5 min) is plotted, thus is only an illustrative display and not a complete result. As shown in Fig. 3, the feature of breathing cycle, whilst clearly observable, was confounded by additional high- and low-frequency components. After a study of the power spectral distribution, a contribution caused by heart contractions was observed to center around frequencies 0.75 and 1.16, while a low-frequency contribution caused by respiratory motion was limited to absolute values smaller than 0.4Hz. The TOF-based gating appeared to yield stronger respiratory components than nonTOF according to the higher SNR observed in Fig. 3. Fig. 4 demonstrates the 1D respiratory traces obtained by COM and PCA algorithms based on nonTOF and TOF data (showing 25 seconds out of 300 seconds of data with hardware-driven signals). The trigger error and frequency/number of large discrepancy Δt over the studied signal were evaluated. The correlation of the TOF PET data-driven signal with respect to Anzai signal (end-inhalation) were computed, compared with the signal generated using nonTOF data. The results are listed in Table I.

Both the TOF and nonTOF data-driven gating obtained good correlations with the Anzai trigger (larger than 0.9). However, the gating with nonTOF data was more likely to generate trigger with large (> 400ms) discrepancy than TOF gating for both COM and PCA algorithms, as shown in Fig. 4. Table I shows that the gating with COM algorithm applied on TOF PET data yielded the best performance in terms of both correlation with 'real' trace and detection accuracy of the respiratory triggers. Although COM was relatively robust in data-driven gating for both datasets, the performance of respiratory gating using TOF information was improved more significantly by PCA compared with COM. For example, the correlation with real trace was increased by 3.47% and 21.45% for COM and PCA method, respectively. This can be expected, since the core idea of PCA is to detect the variation of sinogram pattern, instead of the total counts of the sinogram, and consequently works better on sinograms in higher SNR.

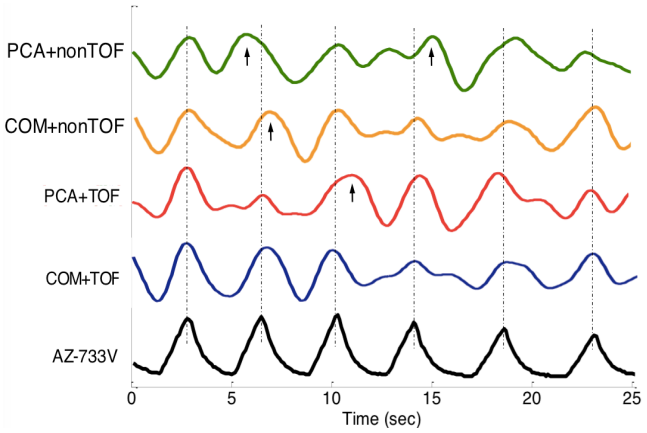

Fig. 4. NonTOF and TOF data-derived respiratory signals obtained by COM and PCA methods with Anzai signal as golded truth and its 6 triggers (dash line). Arrows refer to the trigger with discrepancy larger than 400ms.

IV. Conclusion

In this paper, we proposed and evaluated a novel method for extraction of respiratory signal from TOF PET data. In this method, 3D TOF PET data were rebinned into 2D nonTOF data without loss of TOF information using FORET algorithm. The performance of TOF PET data-driven gating compared with Anzai signal and nonTOF PET data-driven signal was assessed in terms of correlation of respiratory traces and accuracy of detected triggers. Results exhibited that while both datasets yielded good detection accuracy, PET list mode data-driven respiratory signal using TOF information provide superior performance to traditional (nonTOF) method for both COM and PCA in low dose PET/CT study. The results indicate that COM might be more robust under noisy conditions, but this would need to be confirmed after additional evaluation. More in vivo studies are underway to characterize inter-patient variation of breathing patterns.

References

[1] C. Cohade, M. Osman, L. N. Marshall, and R. N. Wahl, "PET-CT: accuracy of PET and CT spatial registration of lung lesions," *Eur J Nucl Med Mol Imaging,* vol. 30, no. 5, pp. 721-6, May, 2003.

[2] S. A. Nehmeh, and Y. E. Erdi, "Respiratory motion in positron emission tomography/computed tomography: a review," *Semin Nucl Med,* vol. 38, no. 3, pp. 167-76, May, 2008.

[3] G. Lucignani, "Respiratory and cardiac motion correction with 4D PET imaging: shooting at moving targets," *European journal of nuclear medicine and molecular imaging,* vol. 36, no. 2, pp. 315-319, 2009.

[4] V. Bettinardi, M. Picchio, N. Di Muzio, and M. C. Gilardi, "Motion management in positron emission tomography/computed tomography for radiation treatment planning," *Semin Nucl Med,* vol. 42, no. 5, pp. 289-307, Sep, 2012.

[5] Y. E. Erdi, S. A. Nehmeh, T. Pan, A. Pevsner, K. E. Rosenzweig, G. Mageras, E. D. Yorke, H. Schoder, W. Hsiao, O. D. Squire, P. Vernon, J. B. Ashman, H. Mostafavi, S. M. Larson, and J. L. Humm, "The CT motion quantitation of lung lesions and its impact on PET-measured SUVs," J Nucl Med, vol. 45, no. 8, pp. 1287-92, Aug, 2004.

[6] D. Visvikis, F. Lamare, P. Bruyant, N. Boussion, and C. C. Le Rest, "Respiratory motion in positron emission tomography for oncology applications: Problems and solutions," Nuclear Instruments and Methods in Physics Research Section A: Accelerators, Spectrometers, Detectors and Associated Equipment, vol. 569, no. 2, pp. 453-457, 2006.

[7] S. Nehmeh, Y. Erdi, C. Ling, K. Rosenzweig, O. Squire, L. Braban, E. Ford, K. Sidhu, G. Mageras, and S. Larson, "Effect of respiratory gating on reducing lung motion artifacts in PET imaging of lung cancer," *Medical physics,* vol. 29, no. 3, pp. 366-371, 2002.

[8] G. Klein, B. Reutter, M. Ho, J. Reed, and R. Huesman, "Real-time system for respiratory-cardiac gating in positron tomography," *Nuclear Science, IEEE Transactions on,* vol. 45, no. 4, pp. 2139-2143, 1998.

[9] M. Dawood, F. Buther, N. Lang, O. Schober, and K. P. Schafers, "Respiratory gating in positron emission tomography: a quantitative comparison of different gating schemes," *Med Phys,* vol. 34, no. 7, pp. 3067-76, Jul, 2007.

[10] L. Boucher, S. Rodrigue, R. Lecomte, and F. Benard, "Respiratory gating for 3-dimensional PET of the thorax: feasibility and initial results," *J Nucl Med,* vol. 45, no. 2, pp. 214-9, Feb, 2004.

[11] S. A. Nehmeh, Y. E. Erdi, C. C. Ling, K. E. Rosenzweig, H. Schoder, S. M. Larson, H. A. Macapinlac, O. D. Squire, and J. L. Humm, "Effect of respiratory gating on quantifying PET images of lung cancer," J Nucl Med, vol. 43, no. 7, pp. 876-81, Jul, 2002.

[12] C. K. McKibben, and N. V. Reo, "A piezoelectric respiratory monitor for in vivo NMR," Magn Reson Med, vol. 27, no. 2, pp. 338-42, Oct, 1992.

[13] S. Vedam, P. Keall, V. Kini, H. Mostafavi, H. Shukla, and R. Mohan, "Acquiring a four-dimensional computed tomography dataset using an external respiratory signal," *Physics in medicine and biology,* vol. 48, no. 1, pp. 45, 2003.

[14] T. Pan, T. Y. Lee, E. Rietzel, and G. T. Chen, "4D-CT imaging of a volume influenced by respiratory motion on multi-slice CT," *Med Phys,* vol. 31, no. 2, pp. 333-40, Feb, 2004.

[15] R. Zeng, J. A. Fessler, J. M. Balter, and P. A. Balter, "Iterative sorting for four-dimensional CT images based on internal anatomy motion," *Med Phys,* vol. 35, no. 3, pp. 917-26, Mar, 2008.

[16] G. Klein, B. Reutter, E. Botvinick, T. Budinger, and R. Huesman, "Fine-scale motion detection using intrinsic list mode PET information." pp. 71-78.

[17] R. A. Bundschuh, A. Martínez-Moeller, M. Essler, M.-J. Martínez, S. G. Nekolla, S. I. Ziegler, and M. Schwaiger, "Postacquisition detection of tumor motion in the lung and upper abdomen using list-mode PET data: a feasibility study," *Journal of Nuclear Medicine,* vol. 48, no. 5, pp. 758-763, 2007.

[18] K. Thielemans, S. Rathore, F. Engbrant, and P. Razifar, "Device-less gating for PET/CT using PCA." pp. 3904-3910.

[19] J. He, G. J. O'Keefe, S. J. Gong, G. Jones, T. Saunder, A. M. Scott, and M. Geso, "A novel method for respiratory motion gated with geometric sensitivity of the scanner in 3D PET," *Nuclear Science, IEEE Transactions on,* vol. 55, no. 5, pp. 2557-2565, 2008.

[20] P. J. Schleyer, M. J. O'Doherty, S. F. Barrington, and P. K. Marsden, "Retrospective data-driven respiratory gating for PET/CT," *Phys Med Biol,* vol. 54, no. 7, pp. 1935-50, Apr 7, 2009.

[21] A. L. Kesner, and C. Kuntner, "A new fast and fully automated software based algorithm for extracting respiratory signal from raw PET data and its comparison to other methods," *Med Phys,* vol. 37, no. 10, pp. 5550-9, Oct, 2010.

[22] M. Conti, B. Bendriem, M. Casey, M. Chen, F. Kehren, C. Michel, and V. Panin, "First experimental results of time-of-flight reconstruction on an LSO PET scanner," *Phys Med Biol,* vol. 50, no. 19, pp. 4507-26, Oct 7, 2005.

[23] S. Cho, S. Ahn, Q. Li, and R. M. Leahy, "Exact and approximate Fourier rebinning of PET data from time-of-flight to non time-of-flight," *Phys Med Biol,* vol. 54, no. 3, pp. 467-84, Feb 7, 2009.

[24] S. Ahn, S. Cho, Q. Li, Y. Lin, and R. M. Leahy, "Optimal rebinning of time-of-flight PET data," *IEEE Trans Med Imaging,* vol. 30, no. 10, pp. 1808-18, Oct, 2011.

[25] M. E. Daube-Witherspoon, and G. Muehllehner, "Treatment of axial data in three-dimensional PET," *J Nucl Med,* vol. 28, no. 11, pp. 1717-24, Nov, 1987.

[26] J. Shlens, "A tutorial on principal component analysis," *arXiv preprint arXiv:1404.1100*, 2014.